



A Comparative Study of Refined and Simplified Thermo-Viscoplastic Modeling of a Thrust Chamber with Regenerative Cooling

Michele Ferraiuolo^a, Vincenzo Russo^a, Kambiz Vafai^{b*}

^a*Structures and Materials Department, Italian Aerospace Research Center (CIRA), Capua, Italy*

^b*Department of Mechanical Engineering, University of California, Riverside, CA 92521, USA*

Abstract

The thermostructural response of the cooling channel of a regeneratively cooled thrust chamber employed for rocket applications can be evaluated by means of analytical and numerical methods. The heat fluxes produced by the combustion inside the thrust chamber cause elevated temperatures in the copper structure composed of ligaments separating the coolant flow from the combustion gases. Those thermal loads together with the mechanical loads due to the flowing coolant and hot gases, lead to a non linear structural response. In the present work a comprehensive study of the viscoplastic phenomena is carried out and a simplified finite element model, which does not take into account strain rate-dependent effects, is adopted.

The aim of the work is twofold: understanding and detail modeling of the thermo-viscoplastic phenomena occurring in the copper inner liner of a rocket thrust chamber and evaluating the degree of importance of strain-hardening rate-dependent phenomena. The present paper demonstrates that the simplified viscoplastic model adopted in this work is suitable in the preliminary design phase since the percentage difference detected with respect to rate dependent models, such as Perzyna's and Robinson's ones, is slightly larger than 10%. Furthermore, this model is particularly useful when the results of strain hardening tests, aimed at evaluating strain rate dependent properties, are not available for the chosen material.

Keywords: Viscoplastic models, Thrust chamber, Thermal ratcheting, Creep

* Tel.: +1 951-827-2135

E-mail address: vafai@engr.ucr.edu

1. Introduction

Liquid Rocket engines for aerospace applications operate at extremely high heat fluxes ($1-10 \text{ MW} / \text{m}^2$) and pressures ($50-100 \text{ bar}$); as a result, the thrust chamber must be actively cooled in order to preserve the hot gas side wall from melting [1], [2]. In particular, regenerative cooling, where the fuel itself acts as a coolant and is passed through the coolant channels, provided in the periphery of the chamber wall, is the most efficient method of cooling since the heat absorbed by the coolant/fuel increases the enthalpy in the cooling channels leading to a more efficient combustion.

Copper alloys are usually chosen for the inner liner of the thrust chamber since they are characterized by high thermal conductivity, which is useful to transfer heat from the combustion chamber to the coolant [3]; moreover, the mechanical properties are sufficient to withstand the thermomechanical cyclic loading encountered in the service life [4]. Since the pressure in the cooling channel is notably above the thrust chamber pressure, the inner liner is under compression, while the outer wall of the chamber is subjected to considerable hoop stresses. Moreover, the material of the inner liner is deteriorated because of the elevated temperatures occurring in the inner wall, and its thermal expansion is constrained by the cold side wall of the liner. As stress and strain levels rise and/or large temperature changes occur, the material behavior may become viscoplastic [5], [6]. The theory of plasticity must be adopted when inelastic material behavior is encountered. Plasticity theories are based on the assumption that material behavior is time independent when load rates are small [7], [8]. On the other hand, material behavior becomes time dependent when quick loading or high temperature values are detected. An example of time dependent inelastic phenomenon is creep. When plastic behavior is coupled with creep and hardening phenomena, viscoplastic models must be taken into account. The temperature at which creep effects become significant when designing thrust chambers is usually about 40% of the melting temperature of the material considered. Creep can be detected at stress values that are always much lower than the strength of the material considered [9], [10].

Viscoplastic behavior of metallic structures are generally studied by means of unified Constitutive models that provide a means of analytically describing the response of a metallic material from the elastic through the plastic range, taking into account strain rate dependent plastic flow, creep, and stress relaxation phenomena. An example of unified viscoplastic method is due to Bodner and Partom [11]. The Bodner-Partom model is a unified model where:

- a flow law is defined to correlate the plastic strain rate with deviatoric stresses,
- a kinetic equation that shows a relationship between the inelastic strain rate to stress invariants taking into account the effects of temperature and internal state variables,
- evolution equations that describe the effects of kinematic and isotropic hardening.

Another unified viscoplastic model which can be found in literature is the Anand model [12]. The Anand model is classified into the group of the unified plasticity models where the inelastic deformation refers to all irreversible deformation that cannot be distinctively separated into the plastic deformation derived from the rate-independent plasticity theories and the part resulting from the creep effect. Compared to the traditional creep approach, the Anand model introduces a single scalar internal variable "s", the resistance to deformation, that is adopted to depict the isotropic resistance to inelastic flow of the material. Another model employed is the Robinson's model, which adopts a dissipation potential to derive the flow and evolutionary laws for the inelastic strain and internal state variables. The model includes only one internal state variable which represents the kinematic hardening. The material behavior is linear elastic for all the stress levels within the dissipation potential and non linear viscoplastic for the stress levels outside.

Porowski proposed an analytical model for evaluating Hot-Gas Wall Deformation and Strain [13]. In this model strain rate dependent effects are considered. Moreover, material properties are assumed not to vary with temperature.

Perzyna's model could be regarded as the first model describing the evolution of viscous effects [14]: it is widely used in many engineering applications, due to the fact that it consists of a reduced number of parameters. A particular feature is that the model allows the stress to get over the Yield surface.

For the above mentioned models, the number of experimental tests needed to characterize the viscoplastic behavior of a metallic structure is quite substantial. Indeed, tensile and compressive tests at different

temperature values as well as strain hardening, creep and relaxation experimental tests should be performed; as a result, the adoption of a simplified viscoplastic model in which a reduced number of experimental data is needed, could be useful in a preliminary design phase when not all the results of the experimental tests are available. For example, the results of strain hardening tests are often not available in the literature. As such, it is valuable to quantify the amount of uncertainty introduced in the finite element model when rate-dependent effects are ignored.

The present paper describes a Finite Element Model to be built in a commercial code (ANSYS) in order to illustrate the highly nonlinear phenomena detected in the hot components of a thrust chamber. Another aim of the present work is to demonstrate that the adoption of a simplified viscoplastic model not taking into account strain rate dependent effects can be useful in a preliminary design phase since it can substantially reduce the computational time needed to run a complex thermostructural analysis.

The structure of this paper is organized as follows: a description of the simplified viscoplastic model, adopted in the finite element analyses, is given in the next section, while the results of the thermostructural analyses conducted on the rocket engines thrust chambers are illustrated in section 3 together with comparisons with test cases taken from literature. In particular, the results of the analyses are aimed at justify that the simplified model can describe the typical phenomena occurring in the inner liner of a regeneratively cooled thrust chamber (dog house effect, thermal ratcheting, etc.). Finally, the conclusions are summarized in section 4.

2. Analysis

2.1. Simplified Viscoplastic model

The current simplified viscoplastic model is composed of the yield criterion, the flow rule, the hardening rule and time-dependent phenomena (creep). To characterize the stress components that induce plasticity, deviatoric stress components are defined by subtracting uniform hydrostatic normal stresses from the stress tensor. The hydrostatic stress is defined as:

$$\sigma_0 = \frac{1}{3}(\sigma_{11} + \sigma_{22} + \sigma_{33}) = \frac{1}{3}\sigma_{ii} \quad (1)$$

while S_{ij} is given by:

$$S_{ij} = \sigma_{ij} - \sigma_0\delta_{ij} \quad (2)$$

The equation given by the von Mises yield criterion identifies a yield surface. If the principal stresses lie within the yield surface, elastic behavior is encountered, while if the principal stresses fall on the yield surface, plastic deformation is detected.

The Prandtl-Reuss flow rule describes the relationship between the plastic strain increment and the deviatoric stresses. In particular, an increment in strain $d\varepsilon$ can be decomposed into an elastic part $d\varepsilon^e$ and a plastic part $d\varepsilon^p$. If the material is isotropic, it can be assumed that the plastic strain increments $d\varepsilon_{ij}^p$ are related to the deviatoric stresses S_{ij} :

$$\dot{\varepsilon}_{ij}^p = \lambda S_{ij} \quad (3)$$

To establish an accurate relationship, one must identify the positive constant scalar λ , which is a plastic multiplier that determines how much plastic strain occurs and depends on the yield criterion and the possible

hardening behavior. When the material is unloaded a new elastic limit, greater than the initial elastic one, will be detected. Due to the hardening phenomenon, a new elastic limit in compression, smaller than the initial one, is encountered. This phenomenon is referred to as Bauschinger effect [15]. Creep is modelled by means of the Norton's law which represents the portion of the creep curve where the creep rate remains almost constant (secondary or steady creep):

$$\dot{\varepsilon} = B\sigma^r \quad (4)$$

where:

- B and r are material constants, r is non dimensional, B is expressed in $[1/s(MPa)^r]$
- $\dot{\varepsilon}$ is the strain rate

2.2. Thrust chamber geometry and boundary conditions

The geometry of the thrust chamber cross section is shown in Figs. 1 and 2, the thermo-mechanical load cycle history is depicted in Fig. 3. Hot gas side adiabatic wall temperature, coolant side bulk temperature with corresponding heat transfer coefficients and pressures are summarized in Table I. The material adopted for the liner is Narloy-Z, while that adopted for the close-out is Electroformed Copper (EF copper). Tables II and III illustrate the thermal and mechanical properties adopted for the thermo-mechanical analyses [16]. The benchmark chosen for the comparison is characterized by relevant creep phenomena. The pressure differential between the coolant and the hot gases flows is 20.68 MPa and the hot phase lasts 240 seconds. As a consequence creep strains are expected to occur in the ligament. The material constants B and r of the Norton's law for the Narloy-Z are:

$$B = 5.12 * 12^{-56} [1/s(MPa)^r]$$

$$r = 6.65$$

The thermal and structural analyses have been conducted on a Finite Element model representing the cooling channel, that is the inner wall, rib and close-out represented in Fig. 4(a). Symmetry conditions have been applied in order to minimize the computational time. The numerical simulation clarifies the influence of the strain rate dependent models on the structural response of the inner liner of the thrust chamber. Moreover, a detailed study on the transient response of the thrust chamber has also been accomplished on the geometry depicted in Fig. 4(b), which is characterized by a lower aspect ratio (height/width). The following analyses were performed:

1. Transient thermal and static structural analysis compared with analytical model results obtained by Porowski [17];
2. Transient thermal and static structural analysis compared with a transient structural analysis on a new configuration characterized by a different aspect ratio;
3. Transient thermal and static structural analysis compared with the results obtained by adopting Robinson's [18] and Perzyna's viscoplastic models [19].

In what follows, the analytical model will be identified as "model 1", while the Robinson's and Perzyna's models will be referred to as "model 2" and "model 3" respectively.

Table provides a summary of the main characteristics of the performed thermostructural simulations. In the

second column the benchmarks with which the results obtained with the current viscoplastic model are compared. In particular, the results of the transient analysis have been compared to those obtained with the corresponding static structural ones.

3. Results and discussions

3.1. Comparison with model 1

A finite element analysis has been conducted adopting the simplified viscoplastic model described in the previous section. The results have been compared with those obtained by Porowski with model 1 [17]. Maximum temperature values (almost 900 K), are detected in the hot gas side of the ligament during the hot phase, as illustrated in Fig. 5(a). With regards to the structural analysis, the deflection of the ligament detected at the end of the thermo-mechanical cycle obtained by the analytical solution and the Finite element models are summarized in Table V. The displacement considered in the Finite Element analysis is the one evaluated in the point illustrated in Fig. 4 (point A). The maximum percentage difference between the current numerical results and the analytical model is about 14%. The effect of the creep phenomena is demonstrated in Fig. 5(b)-(c) where it is clearly visible that the hoop stresses in the ligament decrease with time. In particular, the hoop tangential stresses are compressive during the hot phase, and, as a consequence, the ligament yields in compression. During creep, the hoop stresses relax becoming tensile after about 1 second. The tensile stress is induced because the high temperatures occurring during the hot phase yields in compression of the ligament of the cooling channel and, then, the ligament width is invariably decreased. However, the ribs act as boundaries that prohibit the ligament from decreasing in length as the temperature decreases, so that a tensile stress develops as the material cools. Moreover, since the hoop stresses become tensile before the end of the hot phase, creep rupture damage is a potential failure mode that should be included in the failure analysis.

The current model can reproduce cyclic hardening and thermal ratcheting phenomena, that is cumulative inelastic deformation that can be detected in a structure subjected to thermal cyclic loading. Fig. 6 shows the tangential stress variation with total tangential strain for point A shown in Fig. 4. It is clear the effect of creep during the hot phase; at the end of each cycle residual tensile stresses are encountered leading to thermal ratcheting phenomena. The number of cycles to failure is evaluated by means of Eq. 5 according to Riccius et al. [20], [21]:

$$N = \frac{\varepsilon_u}{\max(0, (\varepsilon_e - \varepsilon_b))} \quad (5)$$

where ε_e is the remaining strain after the considered cycle, ε_b is the strain at the beginning of the considered cycle and ε_u is the ultimate strain of the combustion chamber wall material. Negative strains (compression mode) are not taken into account.

The number of cycles to failure is 44, while 49 cycles were calculated in model 1. As such a 10% difference is detected between the two models when evaluating the service life of the thrust chamber. If creep is not modelled, the tangential stresses during the hot phase remain constant (no stress relaxation phenomena), and, as a consequence, no residual tensile stresses will occur. The number of cycles to failure would be significantly greater if compared to the test case where creep is modelled. Fig. 7 shows the equivalent creep strain contour plots after 1 second and 240 seconds of creep. As expected, creep occurs almost exclusively in the ligament where higher temperature values are detected.

Fig. 8(a) shows the tangential stress variation with time for points A and B. It is clear that the effects of creep are relevant in the first 5-10 seconds (see the grey rectangles in the figure) of the hot phase where the temperature in the ligament rapidly reaches the steady state values. Point B is characterized by higher compressive stress values since temperatures are 150 K to 200 K higher than the values detected in Point A. The tensile tangential stress at the end of the cycles increases cycle after cycle because of the hardening effects

occurring when the ligament is thermo-mechanically loaded.

Fig. 8(b) illustrates the thickness decrease of the ligament as a function of the number of cycles. The deformed shape of the ligament shows the bulging out as a result of the thermo-mechanical load cycles. Our results qualitatively replicated the so-called “dog-house” effect and the thinning of the coolant-channel wall; this effect was caused by the pressure differential acting across the coolant-channel wall.

A transient structural analysis was also carried out. No significant differences were detected between the static and the transient results (the maximum percentage difference is equal to 0.01%). Since the results are very similar, no thermal and structural contour plots will be shown.

3.2. Thermostructural transient analysis

As explained earlier, a less stiff structure, where the ratio between the length of the ligament and the rib width is considerably higher, was examined. This kind of channel is more deformable. The deflection in the centerline, with the same thermomechanical load, is higher with respect to the previous configuration. Therefore, the inertial effects on the structure should not be neglected. The aspect ratio in Geometry 2 is equal to 0.37, that is half the aspect ratio of Geometry 1. A reduced hot phase (2 seconds) has been considered in order to limit the computational time needed to perform the transient structural analysis. Fig. 9 shows the tangential stress distribution at the end of the cycle for the static and the transient analysis. The maximum percentage difference is about 56% and is detected at point B at the end of the first cycle (see also Tables VI and VII). The location of points A and B is shown in Fig. 9. As expected, in the cold phase at the end of the thermomechanical cycle the results of the static analysis become very different with respect to those evaluated with the transient analysis; in fact, when the ligament is rapidly cooled, inertial effects cannot be neglected. Similar considerations could be made when considering the beginning of the hot phase when the ligament is rapidly heated by the combustion gases inside the thrust chamber. The static analysis underestimates the tangential stresses. As such it is inappropriate to refer to the static analysis in the design phase of a thrust chamber. The computational time required for the transient analysis is large, and, as a result, parallel computing is desired.

3.3. Comparison with models 2 and 3

A comparison with the results obtained by means of FE models, where model 2 and model 3 are implemented, based on the geometry of the thrust chamber shown in Fig. 2. The thermomechanical load cycle applied is characterized by a short cycle in which the hot phase lasts 0.8 seconds. The temperature and pressure loading histories together with the material parameters obtained with model 2 can be found in Arya and Arnold [22], while the material parameters adopted for model 3 can be found in [19] and [23]. The analysis results relating to model 3 have been accomplished by means of ANSYS code.

Table VIII shows the thinning of the ligament evaluated at the end of each of the first four cycles. The maximum percentage difference is detected at the end of the third cycle (see Table IX).

The results of the analysis performed adopting model 3 is compared with those obtained with the simplified viscoplastic model. The results show that the maximum percentage difference between the two models is about 12% and occurs at point B at the end of the thermo-mechanical cycle (see Tables X, XI, XII, and XIII).

4. Conclusions

A comprehensive study on the finite element modeling of complex thermo-viscoplastic and transient phenomena occurring in the inner liner of copper alloy thrust chambers employed for aerospace applications was carried out. In particular, a simplified viscoplastic model not taking into account strain hardening rate dependent effects has been adopted. The results have demonstrated that this model is able to reproduce the “dog-house effect” and the ligament thinning that affect the inner lining of the chamber. Furthermore, the structural inertia effects have been taken into account when a less rigid structure is examined. Finally, the results of the current viscoplastic model were compared with more detailed models, such as Robinson’s and Perzyna’s ones, taking into account the strain rate dependent laws. The maximum percentage difference amongst these

models was about 13% and it occurs in the coolant side of the ligament, which is not the most critical point. As such, the adopted simplified model could be successfully employed in a preliminary design phase of a thrust chamber since it substantially reduces the required computational time

References

- [1] Quentmeyer, R. J., "Experimental Fatigue Life Investigation of Cylindrical Thrust Chambers," NASA TM X-73665, 1977.
- [2] Armstrong, W. H., "Structural Analysis of Cylindrical Thrust Chamber," Vol. I, Final Rept., NASA Lewis Research Center, NASA-CR-159552, Contract NASA-21361, March 1979
- [3] Arya, V. K., Halford, G. R., Finite Element Analysis of Structural Engineering Problems Using a Viscoplastic Model Incorporating Two Back Stresses. Proceedings of Int. Seminar on Inelastic Analysis, Fracture and Life Prediction, Paris, France, 1993 and NASA TM-106046, 1993
- [4] Freed, A. D., "Structure of a Viscoplastic Theory," Constitutive Equations and Life Prediction Models for High Temperature Applications Symposium, NASA Lewis Research Center, NASA TM-100749, sponsored by American Society of Mechanical Engineers, Berkeley, CA, June 1988.
- [5] Arya, V. K., Analytical and Finite Element Solutions of Some Problems Using a Viscoplastic Model Journal of Computers and Structures, 33,4, 957-967, 1989.
- [6] Tsung-Yu Pan, Thermal Cycling Induced Plastic Deformation in Solder Joints—Part I: Accumulated Deformation in Surface Mount Joints, J. Electron. Packag. 113(1), 8-15 (Mar 01, 1991)
- [7] Kelly, P., Solid Mechanics, Part II, Lecture notes, The University of Auckland
- [8] Karayaka, M., Huseyin S., Thermo-Mechanical Fatigue of Metal Matrix Composites, Low Cycle Fatigue and Elasto-Plastic Behaviour of Materials—31992, pp 13-18
- [9] Weronski, A., Hejwowski T., Thermal fatigue of metals, AIAA Education series, 1991
- [10] Earl A. Thornton, Thermal structures for aerospace applications, AIAA Education Series (1996).
- [11] Bodner S. R. and Partom Y., Constitutive Equations for Elastic-Viscoplastic Strain-Hardening Materials, J. Appl. Mech. 42(2), 385-389 (Jun 01, 1975)
- [12] Wang, G. Z., Cheng, Z. N., Becker K., Wilde, J., Applying Anand Model to Represent the Viscoplastic Deformation Behavior of Solder Alloys, J. Electron. Packag. 123(3), 247-253 (Oct 20, 1998)
- [13] Calladine, C. R. , "A Rapid Method for Estimating the Greatest Stress in a Structure Subjected to Creep," Proc. Instn, Mech. Engr. , Vol 178,1963-64.
- [14] Ambroziak, Klosowski, Nowicki, Schmidt, Implementation of continuum damage in elast-viscoplastic constitutive equations
- [15] Yoshida, F., Uemori, T., A model of large-strain cyclic plasticity describing the Bauschinger effect and work hardening stagnation, International Journal of Plasticity Volume 18, Issues 5–6, October 2002, Pages 661–686
- [16] Esposito, J.J., Zabora, R.F., "Thrust Chamber Life Prediction - Mechanical and Physical Properties of High Performance Rocket Nozzle Materials," NASACR-134806, Contract NAS3-17838, NASA-Lewis Research Center, Cleveland, Ohio, March 1975.
- [17] Porowski, J. S., O'Donnell, W. J., Badlani, M. L., and Kasraie, B., "Simplified Design and Life Prediction of Rocket Thrust Chambers", Journal of Spacecraft and Rockets, Vol. 22, No. 2, 1985, pp.181-187.
- [18] Arya, V. K.; and Kaufman, A.: Finite Element Implementation of Robinson's Viscoplastic Model and Its Application to Some Uniaxial and Multiaxial Problems. J. Eng. Comput., vol. 6, no. 3, 1989, pp. 537-547.
- [19] Radial lip seal simulation using ANSYS non-standard procedures, Wang, Draper, odapp, Emerson Climate Technology
- [20] Riccius, J.R., Hilsenbeck, M.R. and Haidn, O.J., "Optimization of geometric parameters of cryogenic liquid rocket combustion chambers," 37th AIAA/ASME/SAE/ASEE JPC, AIAA-01-3408, 2001
- [21] Riccius, J.R., Haidn, O.J. and Zametaev, E.B., "Influence of time dependent effects on the estimated life time of liquid rocket combustion chamber walls," AIAA 2004-3670, 40th AIAA/ASME/SAE/ASEE Joint Propulsion Conference, July 2004 Fort Lauderdale, Florida
- [22] Arya, V. K., and Arnold, S. M., "Viscoplastic Analysis of an Experimental Cylindrical Thrust Chamber Liner," AIAA Journal, 1992, Vol. 30, No. 3, 1992, pp. 781-789
- [23] Kalpakjian S. and Schmid S.R., Manufacturing Processes for Engineering Materials, 5th ed., 2008, Pearson Education ISBN No. 0-13-227271-7

Table I: Thermomechanical cycle coefficients

	Cold	Hot
Hot-gas side Heat transfer coefficient (W/m ² K)	0	26670
Hot-gas side wall Temperature (K)	278	3290
Pressure differential (Mpa)	20.57	20.67
Coolant side Heat transfer coefficient (W/m ² K)	120000	40180
Coolant side bulk Temperature (K)	57	57

Table II: Thermal and physical properties – Narloy Z

Thermal Conductivity (W/mK)	295
Density (kg/m ³)	9134
SpecificHeat (J/kgK)	373
Coefficient of thermal expansion (1/K)	17.2*10 ⁻⁶

Table III: Mechanical properties - Narloy Z

	27 K	294 K	533 K	810 K
Modulus of Elasticity (Gpa)	143	128	113	87
Tensile Yield (Mpa)	228	194	168	87
Tensile Strength (Mpa)	250	220	190	135
Poisson's ratio	0.34	0.34	0.34	0.34

Table IV: Summary of the performed thermostructural analyses

Analysis	Benchmark	Geometry	Analysis type	Hot phase length (seconds)	Cycles analyzed
1	Model 1	1	static	240	4
2	Corresponding static analysis	2	transient	2	1
3	Model 2 and 3	1	static	0.8	4

Table V: Ligament deflection for FE and analytical models

Analytical solution [m]	Simplified FE model (Ansys) [m]
7.4*10 ⁻⁶	8.45*10 ⁻⁶

Table VI: Tangential stresses - hot phase - creep after 1.2 seconds

	Static analysis [MPa]	Transient analysis [MPa]	Percentage difference
Point A	74.9	74.7	0.27 %
Point B	-97	-96.2	0.83 %

Table VII: Tangential stresses –cold phase –end of the first cycle

	Static analysis [MPa]	Transient analysis [MPa]	Percentage difference
Point A	321	391	-17.90 %
Point B	217	139	56.12 %

Table VIII: Thinning (mm) of the ligament at the end of the first 4 cycles

	Model 2	Simplified model	Model 3
I cycle	1.80e-2	1.78e-2	2.04e-2
II cycle	2.10e-2	2.03e-2	2.07e-2
III cycle	2.20e-2	2.54e-2	2.24e-2
IV cycle	2.37e-2	2.67e-2	2.45e-2

Table IX: Percentage difference of the simplified model with respect to models 2 and 3

	Percentage difference with model 2	Percentage difference with model 3
I cycle	1.12	12.7
II cycle	3.45	1.9
III cycle	-13.39	-13.4
IV cycle	-11.13	8.9

Table X: Point A - Von Mises Stress and Equivalent plastic strain at the end of the hot phase (1.8 seconds)

Point A (1.8 seconds)	Simplified model	Model 3	Percentage difference
von Mises stress	66.0	72.9	-10.5
Equivalent plastic strain	0.0117	0.0118	-0.9

Table XI: Point A - Von Mises Stress and Equivalent plastic strain at the end of the cycle (3.5 seconds)

Point A (1.8 seconds)	Simplified model	Model 3	Percentage difference
von Mises stress	197.0	211.6	-7.4
Equivalent plastic strain	0.0242	0.0241	0.4

Table XII: Point B - Von Mises Stress and Equivalent plastic strain at the end of the hot phase (1.8 seconds)

Point A (1.8 seconds)	Simplified model	Model 3	Percentage difference
von Mises stress	111.2	123.4	-11.0
Equivalent plastic strain	0.0258	0.0118	5.4

Table XIII: Point B - Von Mises Stress and Equivalent plastic strain at the end of the cycle (3.5 seconds)

Point A (1.8 seconds)	Simplified model	Model 3	Percentage difference
von Mises stress	234.7	263.7	-12.4
Equivalent plastic strain	0.0393	0.0377	4.1

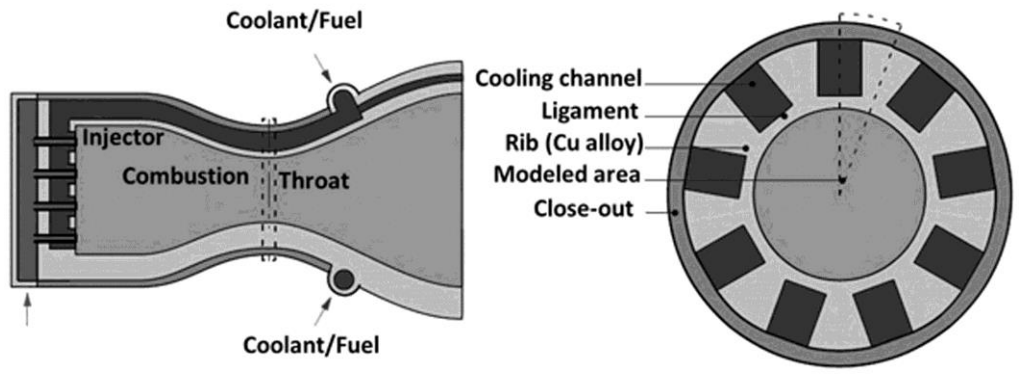


Fig. 1: Scheme of the regenerative liquid rocket engine

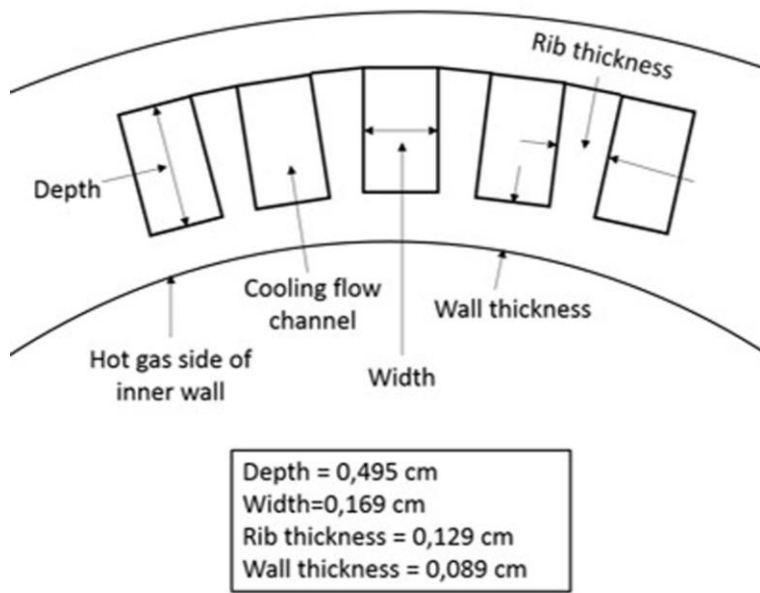


Fig. 2: Cooling channel geometry

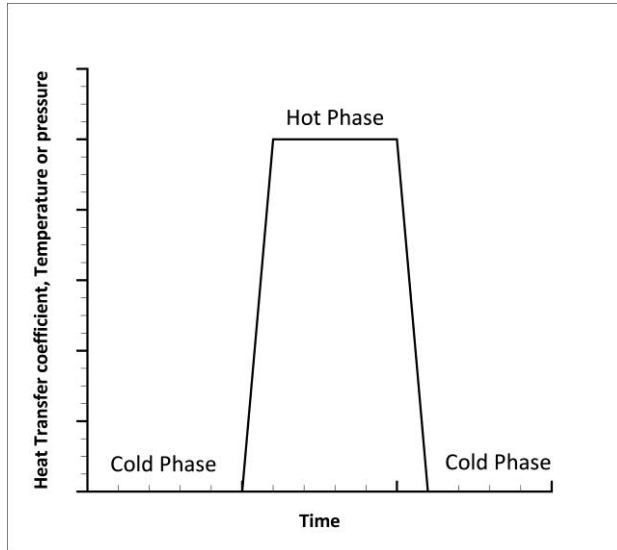


Fig. 3: Thermomechanical load cycle

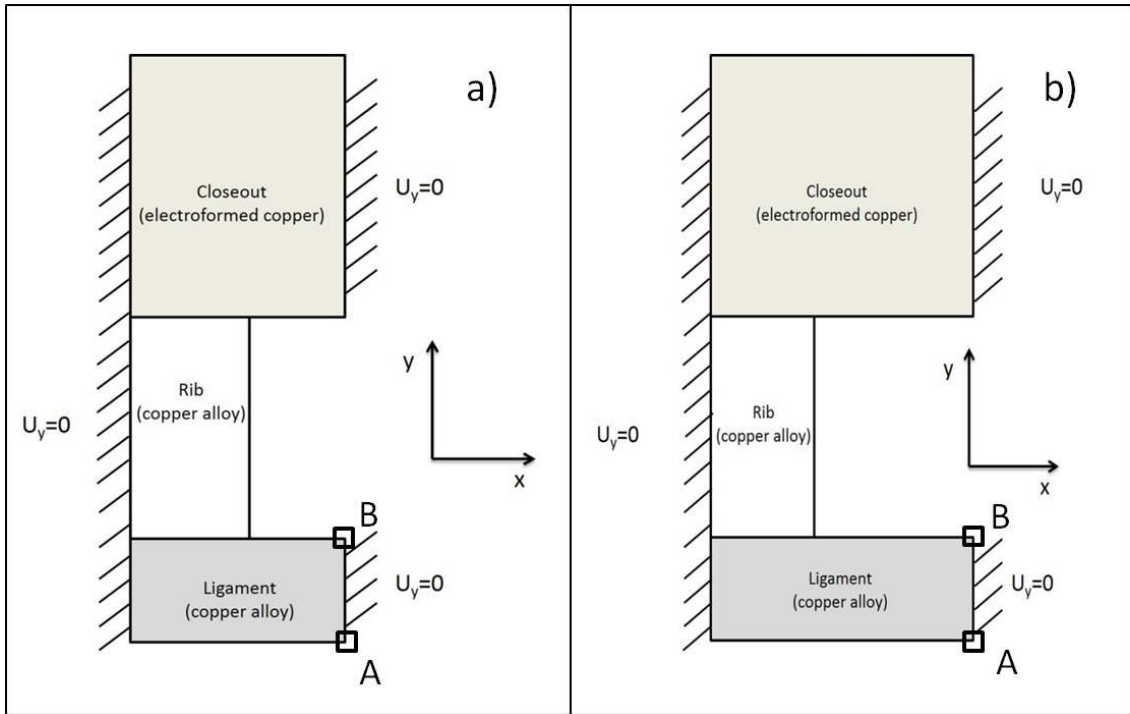


Fig. 4: Cooling channel model adopted in ANSYS (a): Geometry 1, (b): Geometry 2

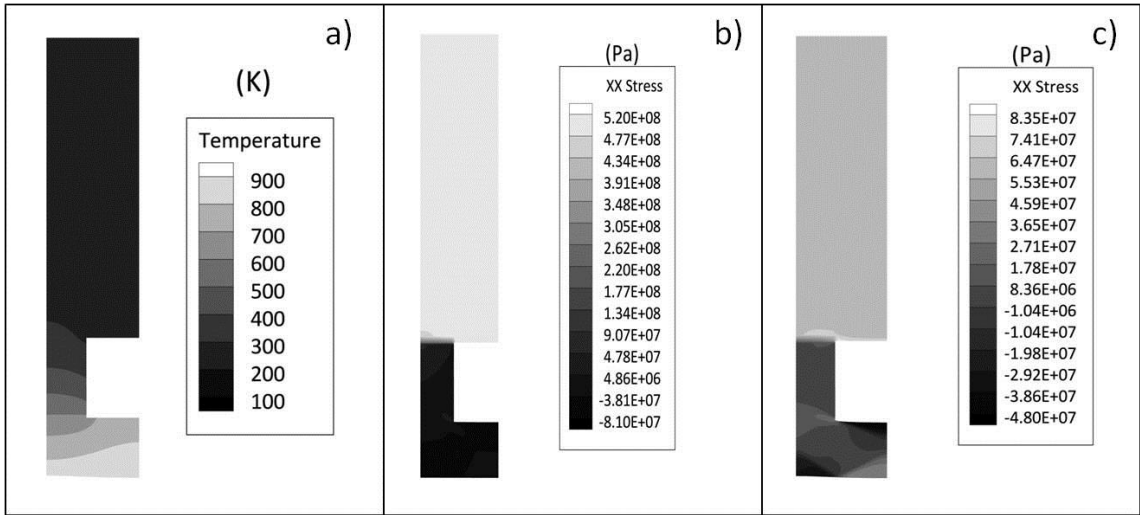


Fig. 5: (a): Temperature contour plot (Hot phase), (b): Hoop tangential stress (creep after 1 second), (c): Tangential stress - creep after 240 seconds

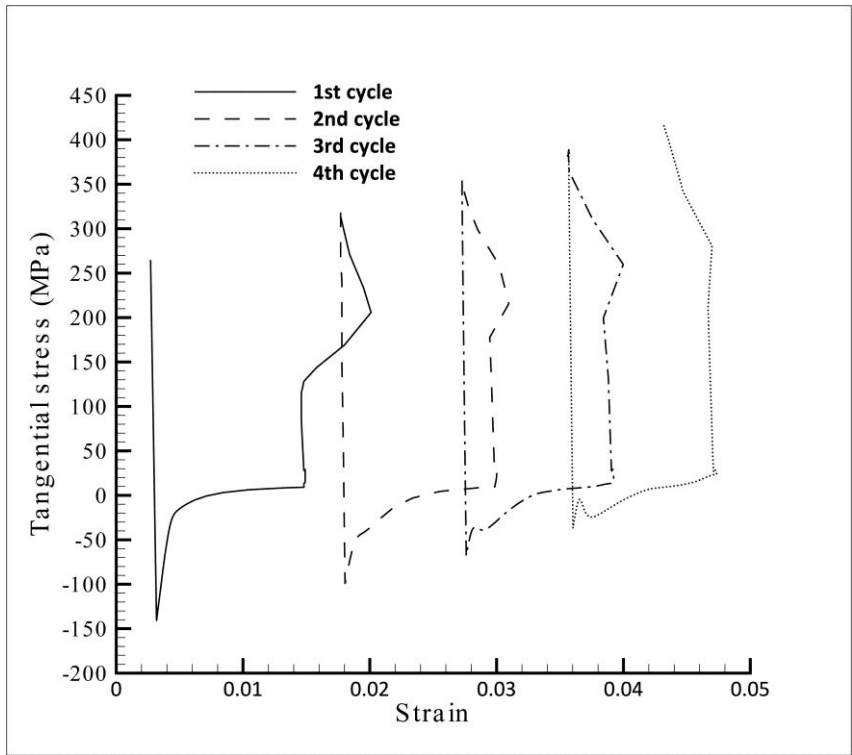


Fig. 6: Tangential Stress vs Total tangential strain - 4 cycles

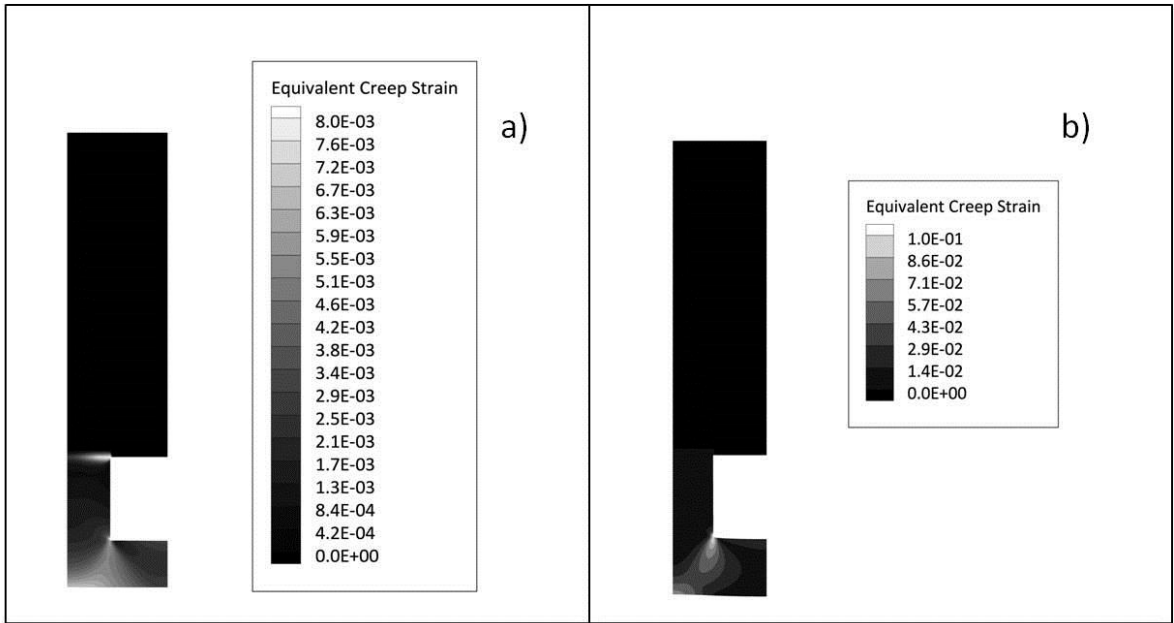


Fig. 7: Equivalent creep strain, (a): creep after 1 second, (b): creep after 240 seconds

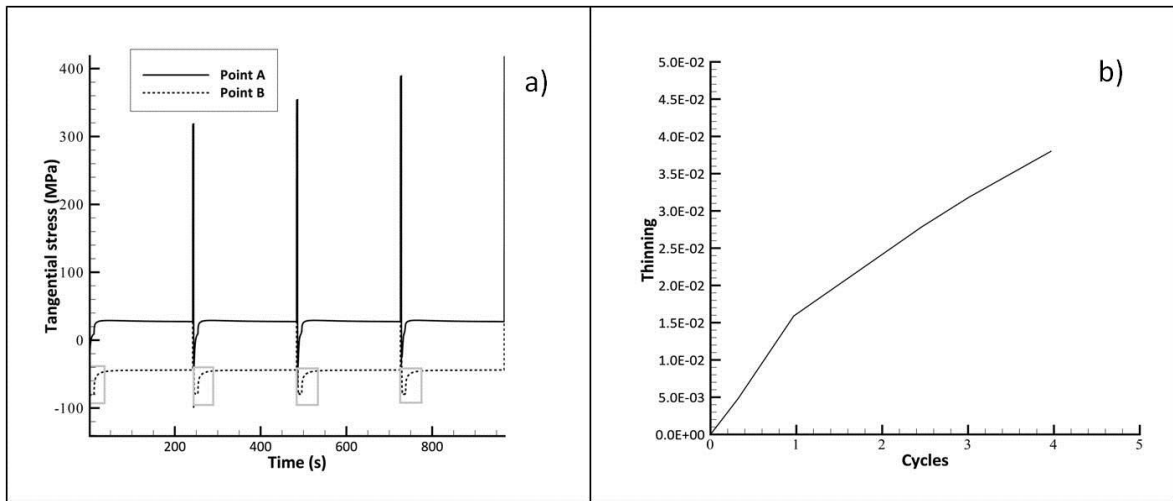


Fig. 8: (a): Tangential stress vs time for points A and B, (b): Decrease in radial thickness - segment AB

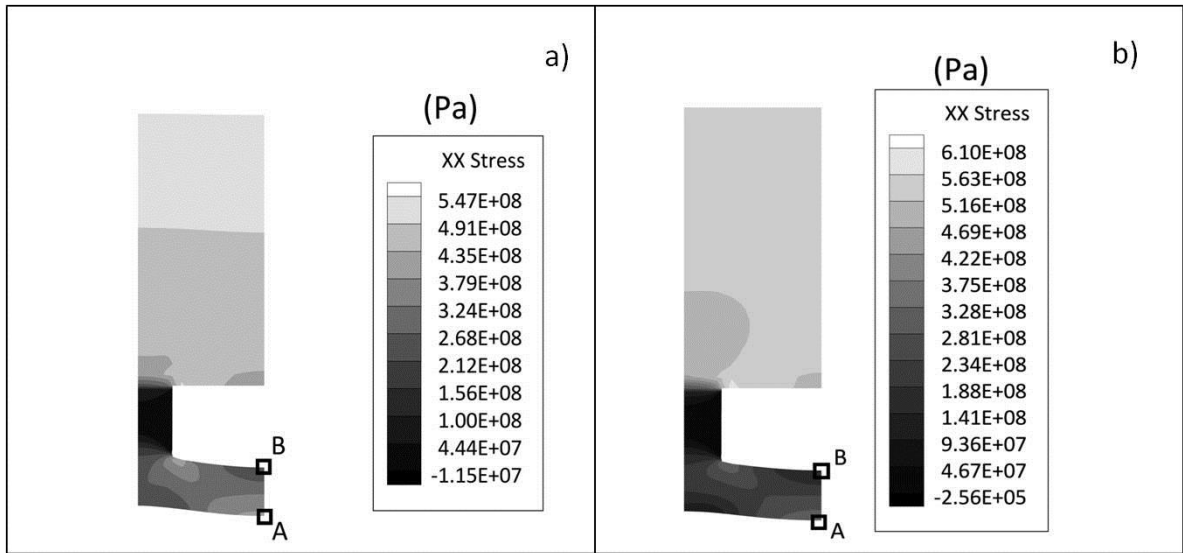


Fig. 9: Tangential stresses at the end of the cycle, (a): static structural analysis, (b): transient structural analysis

